IIETA International Information and Engineering Technology Association
Advancing the World of Information and Engineering

Annales de Chimie - Science des Matériaux
Vol. 50, No. 3, June, 2026, pp. 241-252
Journal homepage: http://iieta.org/journals/acsm

Fabrication and in Vitro Evaluation of a ZnO-Reinforced Co-Amoxiclav-Loaded PP/PLA Composite Suture Containing Collagen and Chitosan

Ruqaya K. Jabir*, Auda J. Braihi, Ali A. A. Al-Zubiedy

Department of Polymer Engineering and Petrochemical Industries, College of Materials Engineering, University of Babylon, Babylon 51001, Iraq

Corresponding Author Email: ruqaya2694@gmail.com

https://doi.org/10.18280/acsm.500304

Received: 13 April 2026
Revised: 12 June 2026
Accepted: 20 June 2026
Available online: 30 June 2026

Keywords:
polypropylene/poly (lactic acid) composite suture, ZnO nanoparticles, Co-Amoxiclav loading, collagen/chitosan additives, antibacterial activity, in vitro drug release

ABSTRACT

Polypropylene (PP) sutures are widely used because of their chemical stability, flexibility, and mechanical strength, but their hydrophobicity and limited surface bioactivity restrict functional performance. This study fabricated a zinc oxide (ZnO)-reinforced Co-Amoxiclav-loaded PP/poly (lactic acid) (PLA) composite suture containing Polypropylene-grafted maleic anhydride (PP-g-MA), collagen, chitosan, polyethylene glycol (PEG), and PVP-assisted drug loading. The selected formulation consisted of a 50/50 PP/PLA matrix with 2 wt.% PP-g-MA, 5 wt.% collagen, 2 wt.% chitosan, 2.5 wt.% PEG, and 1.5 wt.% ZnO. Compared with pure PP, tensile strength increased by 77.4% and elastic modulus by 174.4%, while elongation remained 58.5 ± 0.5%. The selected ZnO formulation showed improved apparent wettability, and the contact angle slightly decreased from 50.285° to 48.8° after loading. Field-emission scanning electron microscopy (FESEM) /Energy-dispersive X-ray spectroscopy (EDX) and Fourier transform infrared spectroscopy (FTIR) supported ZnO incorporation and mainly physical drug deposition. The loaded suture showed progressive amoxicillin-equivalent release over 8 h, higher at pH 5.2 than pH 7.3. Phosphate-buffered saline (PBS) immersion produced 60.8% mass loss after 21 days. Antibacterial testing showed visible inhibition zones, with an estimated representative diameter of about 36 mm. Overall, the developed suture showed promising material-level performance, but further validation is required before surgical applicability.

1. INTRODUCTION

Surgical sutures remain among the most commonly used wound-closure materials because they provide temporary mechanical support during tissue approximation and healing [1, 2]. However, conventional sutures may contribute to postoperative complications when their surfaces promote bacterial adhesion, poor tissue interaction, or limited local therapeutic activity [3-5]. Therefore, the development of functional polymeric sutures with improved mechanical performance, antibacterial activity, and drug-delivery capability has attracted increasing attention in biomedical materials research [5, 6].

Polypropylene (PP) is widely used in surgical sutures because of its chemical stability, flexibility, and mechanical strength. Nevertheless, PP is hydrophobic, non-biodegradable, and has limited surface bioactivity. Poly (lactic acid) (PLA), in contrast, is a biodegradable polyester with higher polarity and potential for hydrolytic degradation. Blending PP with PLA may provide a tunable polymer matrix that combines the mechanical stability of PP with the more polar and degradable character of PLA. However, PP/PLA blends are generally immiscible and may show weak interfacial adhesion, phase separation, and reduced mechanical properties if the blend is not properly compatibilized [2, 7-9].

Polypropylene-grafted maleic anhydride (PP-g-MA) can be used as a compatibilizer to improve interfacial interaction and stress transfer between the PP and PLA phases [9]. In addition, collagen and chitosan can be incorporated as functional bio-based additives because they contain polar functional groups and may improve the surface affinity of the suture toward aqueous environments. Chitosan has also been an area of extensive research for its antimicrobial activity and polyethylene glycol (PEG) is used at a suitable concentration to increase flexibility, wettability and processability [10-12]. But, too much hydrophilic or soft component(s) can lead to a loss of tensile strength and dimensional stability, so the formulation needs to be carefully balanced.

Zinc oxide nanoparticles (ZnO NPs) have been incorporated into polymeric biomaterials and coating systems because of their antibacterial activity, surface activity, and potential reinforcing effect [10, 13, 14]. In polymer-composite sutures, zinc oxide (ZnO) may contribute to improved antibacterial behavior and mechanical performance, but its concentration must be controlled because nanoparticle agglomeration can generate stress-concentration points and reduce the efficiency of reinforcement. Moreover, antibiotic loading can further enhance the antibacterial function of the suture surface [6, 15,

16]. A commercial Co-Amoxiclav formulation was used as an amoxicillin-containing antibacterial drug source to evaluate the ability of the developed polymer-composite suture to provide localized amoxicillin-equivalent release. Similar drug-loaded ZnO-based systems have been reported for antibacterial and wound-related applications [17].

Previous studies have reported polymeric surgical sutures [1, 2], antimicrobial and coated sutures [5, 6], nanoparticle-modified sutures [13, 15, 16], and ZnO-containing biomaterial systems [10, 13, 14, 17]. PP/PLA blending and PP-g-MA compatibilization have also been investigated in polymer-blend systems [9], while antibiotic-loaded ZnO-based systems have been explored for local antibacterial delivery [6, 18]. However, limited attention has been given to linking these elements within a single composite suture formulation and evaluating their combined effects on mechanical behavior, surface wettability, drug release, degradation, and antibacterial response.

The novelty of this work lies in developing an integrated PP/PLA-based composite suture in which PP-g-MA compatibilization, collagen/chitosan/PEG functional modification, ZnO reinforcement, and Co-Amoxiclav/PVP-assisted loading are combined within one selected formulation. This approach connects formulation design with structure-property-function evaluation under the tested in vitro conditions, rather than treating polymer blending, nanoparticle incorporation, and drug loading as separate aspects.

Therefore, this study aimed to fabricate and evaluate ZnO-reinforced Co-Amoxiclav-loaded PP/PLA composite sutures. The developed sutures were assessed in terms of mechanical properties, morphology, chemical structure, apparent wettability, amoxicillin-equivalent release, phosphate-buffered saline (PBS) immersion mass-loss behavior, antibacterial activity, photocatalytic response, and preliminary cell response.

2. MATERIALS

PP was supplied by Al-Mohand Company, Iran. According to the supplier information, PP had a density of 0.946 g/cm³, tensile strength of 18 MPa, elastic modulus of 1472 MPa, and thermal stability of 160 ℃. PLA was purchased from Shanghai Macklin Biochemical Technology Co., China, with a molecular weight of approximately 80,000 g/mol, melting point of 158.38 ℃, and particle size of 3 mm. Chitosan was purchased from Shanghai Macklin Biochemical Technology Co., China, with a molecular weight of 500,000 g/mol, degree of deacetylation of 80%, melting point of 107.24 ℃, and loss on drying of 0-10%.

Collagen and PP-g-MA were purchased from Shaanxi Sai Yang Food Co., China. Collagen was supplied as a light yellow to white dry powder with a bulk density of 0.33 g/mL and a pH of 6.6 for a 10% aqueous solution. PP-g-MA had a grafting level of 1.5 wt.%, melting point of 160-165 ℃, and melt flow index of 500 g/10 min. ZnO NPs were obtained from Shanghai Aladdin Co., China, with a purity of ≥99%, molecular weight of 81.39 g/mol, melting point of 1975 ℃, and nominal particle size of <100 nm.

PEG (molecular weight 4000 g/mol) was obtained from HI Media Laboratories Pvt. Ltd., India. Polyvinylpyrrolidone (PVP, molecular weight 3000 g/mol) was used as a solubilizing and loading-enhancing agent during the drug-loading process. The antibacterial agent was obtained from a commercially available Co-Amoxiclav formulation containing amoxicillin 500 mg and clavulanic acid 125 mg per dosage unit. The product was manufactured by LDP TORLAN, India, and purchased from local pharmacies. The formulation was used as the model antibacterial drug source for surface loading of the fabricated sutures. Deionized water was used as the solvent during drug loading. PBS, methylene blue (MB), and other reagents used for release, PBS immersion mass-loss, and photocatalytic tests were of analytical grade unless otherwise stated. All materials were used as received in their supplied dry granular or powder form.

3. FORMULATION SCREENING AND SELECTION OF THE SELECTED COMPOSITION

A stepwise formulation screening procedure was used to select the most suitable polymer-composite suture composition. The stepwise screening procedure was mainly based on tensile strength, total elongation, elastic modulus, and surface wettability, because these responses represent the required balance between mechanical performance and surface behavior for functional polymeric sutures. During the ZnO nanoparticle content-screening step, the 1.5 wt.% ZnO formulation was selected because it provided the best mechanical balance, particularly tensile strength and elastic modulus, while maintaining acceptable elongation and improved wettability. All the contents of PP-g-MA, collagen, chitosan, PEG and ZnO nanoparticles (NPs) are based on the weight of PP/PLA matrix, unless otherwise stated. The entire screening program is outlined in Table 1.

Table 1. Stepwise screening plan for selecting the polymer-composite suture composition

Screening Step	Variable Investigated	Tested Levels	Selection Criterion	Selected Level
Step 1	PP/PLA ratio	100/0, 75/25, 50/50, and 25/75 wt.%	Best balance of TS, TE, E, and CA	50/50 wt.%
Step 2	PP-g-MA content	1, 2, and 4 wt.%	TS and TE	2 wt.%
Step 3	Collagen content	2.5, 5, and 7.5 wt.%	Mechanical performance and CA	5 wt.%
Step 4	Chitosan content	1, 2, and 3 wt.%	TS, E, and CA	2 wt.%
Step 5	PEG content	2.5, 5, and 7.5 wt.%	Strength retention, flexibility, and CA	2.5 wt.%
Step 6	ZnO nanoparticle content	1, 1.5, and 2 wt.%	Highest TS and E with acceptable TE	1.5 wt.%

Note: Additive contents are expressed as wt.% relative to the PP/PLA matrix mass. For example, 2 wt.% PP-g-MA means 2 g PP-g-MA per 100 g of PP/PLA matrix. PP = Polypropylene, PLA = poly (lactic acid); PP-g-MA = Polypropylene-grafted maleic anhydride; TS = tensile strength, TE = total elongation, E = elastic modulus, and CA = contact angle.

In the first step, PP/PLA blends were prepared with different weight ratios to find out an appropriate polymer matrix. The tested PP/PLA ratios were 100/0, 75/25, 50/50, and 25/75 wt.%. The 50/50 PP/PLA blend was chosen for the next stage since it exhibited the best combination of tensile strength, elongation, modulus and wettability amongst the other blends investigated.

To enhance the adhesion of the interface between PP and PLA, PP-g-MA was added in the second step. The influence of the PP-g-MA concentration was investigated and the concentration of 2 wt.% PP-g-MA (based on the matrix mass of PP/PLA) was chosen as it gave the best compromise between tensile strength and elongation of all the tested concentrations. The blend was then sequentially functionalized with collagen, chitosan and PEG as functional additives to enhance surface and mechanical properties of the blend. The combination of 5 wt.% collagen, 2 wt.% chitosan and 2.5 wt.% PEG (all based on the PP/PLA matrix mass) was chosen as the concentration of the additives based on the responses measured.

Finally, the chosen PP/PLA/PP-g-MA/collagen/chitosan/PEG formulation was filled with 1, 1.5 and 2 wt.% (based on the mass of the PP/PLA matrix) of ZnO NPs. The formulation with 1.5 wt.% ZnO NPs was found to be the selected formulation as it has the maximum tensile strength and elastic modulus and still has acceptable elongation among the different levels of ZnO tested. Hence, the composition for further drug loading and functional evaluation was 50/50 PP/PLA matrix, 2 wt.% PP-g-MA, 5 wt.% collagen, 2 wt.% chitosan, 2.5 wt.% PEG and 1.5 wt.% of ZnO NPs (all based on PP/PLA matrix mass).

4. FABRICATION OF POLYMERIC SURGICAL SUTURES

The selected PP/PLA-based formulations described in Section 3 were processed using a locally designed laboratory-scale piston-driven monofilament extrusion system, as shown in Figure 1.

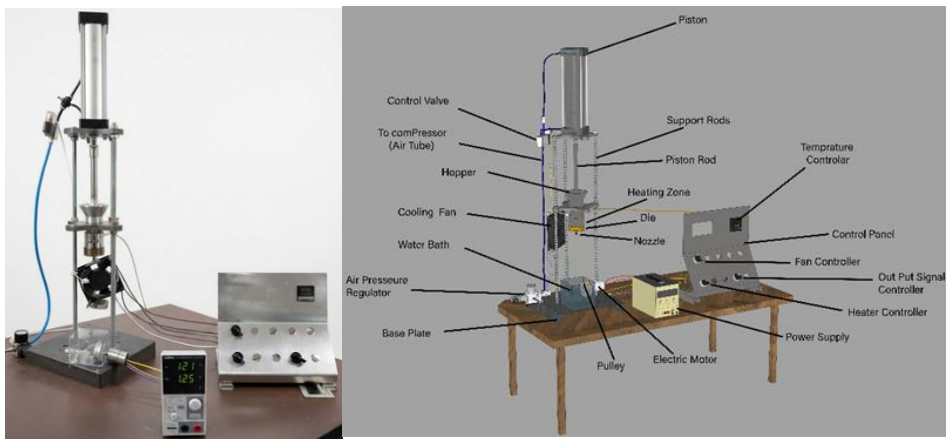

(a) (b)

Figure 1. Locally designed laboratory-scale piston-driven monofilament extrusion system used for fabricating polymeric composite sutures: (a) photographic image of the experimental setup, (b) 3D AutoCAD model of the extrusion system

It was comprised of a hopper, a heated barrel, a piston mechanism, a shaping die, a water-cooling bath, a pneumatic pressure regulator and a motorized winding unit. The base formulation included 50/50 PP/PLA matrix with 2 wt.% PP-g-MA, 5 wt.% collagen, 2 wt.% chitosan and 2.5 wt.% PEG, all the percentages are based on the PP/PLA matrix. To prepare the reinforced composite suture candidates, this selected formulation was reinforced with 1, 1.5 and 2 wt.% of ZnO NPs based on the mass of the PP/PLA matrix.

The as-received dry components were manually premixed to obtain a preliminary dry blend before extrusion. The mixture was then fed into the heated barrel of the extrusion system. The extrusion temperature was maintained at 180 °C, and the heating rate was set at 10 °C/min. After reaching the processing temperature, the molten blend was held in the heating chamber for approximately 3 min before extrusion.

The molten material was extruded through a shaping die with an outlet diameter of approximately 0.4 ± 0.05 mm. After extrusion, the filament was continuously cooled in a water bath and drawn using the motorized winding unit at a linear speed of 700-750 mm/min, which reduced and stabilized the filament diameter. The total extrusion process required approximately 10 min for each formulation. The obtained continuous filaments had an average final diameter of 0.35 ± 0.05 mm, as measured using a vernier caliper, and were collected for subsequent drug loading and characterization.

5. DRUG LOADING PROCEDURE

The selected ZnO-reinforced composite suture formulation was used for the drug-loading step. The fabricated sutures were cut into uniform segments of approximately 5 cm in length. Before drug loading, the suture segments were exposed to ultraviolet (UV) irradiation for 30 min to reduce initial surface contamination. After UV exposure, the fibers were visually inspected, and no apparent discoloration, loss of flexibility, surface damage, or morphological deterioration was observed.

The loading solution was prepared by dissolving 0.75 g of the commercial Co-Amoxiclav formulation and 3.0 g of PVP (molecular weight 3000 g/mol) in 100 mL of deionized water. The Co-Amoxiclav formulation contained amoxicillin 500 mg and clavulanic acid 125 mg per dosage unit and was used as the antibacterial drug source. PVP was used as a solubilizing and loading-assisting polymer to improve the dispersion of the drug formulation in the aqueous medium.

The prepared solution was first homogenized using a

magnetic stirrer at moderate speed for 30 min. It was then sonicated in an ultrasonic water bath for 2 h to improve dissolution and reduce possible aggregation of the drug/PVP components. The UV-treated suture segments were fully immersed in the prepared loading solution in a glass flask for 3 h at room temperature without agitation. After impregnation, the sutures were removed from the solution and dried in a laboratory oven at 45 °C for 10 min to remove residual solvent. The obtained Co-Amoxiclav-loaded composite sutures were stored in clean containers for subsequent characterization, release testing, antibacterial evaluation, and biological assessment.

The exact drug loading capacity and loading efficiency were not directly quantified in this study. Therefore, the subsequent release profile is interpreted as the cumulative amoxicillin-equivalent release from the Co-Amoxiclav-loaded suture under the tested conditions, rather than as a percentage of the total drug initially loaded into the suture.

6. CHARACTERIZATION AND EVALUATION METHODS

The fabricated polymer-composite sutures were characterized using mechanical, morphological, chemical, wettability, antibacterial, drug-release, PBS immersion mass-loss, photocatalytic, and cell-based biological tests. The analyses were performed on representative specimens from the selected formulations, and the results were reported as mean ± standard deviation where applicable. The main characterization and experimental analyses were conducted at Nawat Al-Olom Scientific Ltd. Co., Phi Nano Science Center, Baghdad, Iraq.

6.1 Mechanical testing

The tensile properties of the fabricated monofilament sutures were evaluated using a universal testing device (Instron 5556, type WDW/5E) according to ASTM D3822, which is appropriate for single-fiber and monofilament-type tensile testing. A load cell of 0.05 kN was used. The gauge length was 25 mm, and the crosshead speed was 15 mm/min, corresponding to an elongation rate of 60% of the initial gauge length per minute. The final suture diameter used for stress calculation was measured using a vernier caliper, as described in Section 4. During testing, no slippage was observed, the stress-strain curves were smooth, and the specimens fractured approximately within the middle region of the gauge length rather than near the grips. Each test was repeated three times, and the results were reported as mean ± standard deviation.

6.2 Morphological and chemical characterization

The surface morphology of the unloaded and Co-Amoxiclav-loaded ZnO-reinforced composite sutures was examined using field-emission scanning electron microscopy (FESEM; SIGMA VP, Carl Zeiss, Germany) at 50,000× magnification. Energy-dispersive X-ray spectroscopy (EDX) was used to examine the elemental composition of the analyzed surface regions and to confirm the presence of ZnO-related elements before and after drug loading.

Fourier transform infrared spectroscopy (FTIR) was performed using a PerkinElmer FTIR spectrometer (PerkinElmer Inc., USA). FTIR spectra were recorded to identify the characteristic functional groups of the composite suture components and to evaluate possible interactions after Co-Amoxiclav loading.

6.3 Surface wettability measurement

Surface wettability was evaluated by water contact-angle measurement using a locally manufactured contact-angle device in Baghdad, Iraq. The contact angle was measured using the low-bond axisymmetric drop-shape analysis (LBADSA) method. A distilled-water droplet of approximately 2.75 μL was placed on the suture surface, and the droplet profile was recorded using a charge-coupled device (CCD) camera at 35 frames/s. The reported values represent the average of seven measurements taken at different positions on the sample surface.

6.4 Antibacterial activity and drug-release evaluation

The antibacterial activity was evaluated against Staphylococcus aureus and Escherichia coli using the agar diffusion method. Mueller-Hinton agar was prepared, sterilized at 121 °C for 15 min, poured into sterile Petri dishes, and inoculated with the bacterial strains. Equal lengths of the unloaded and Co-Amoxiclav-loaded sutures were placed on the inoculated agar plates and incubated for 24 h at 37 °C. The antibacterial response was assessed based on the formation of visible inhibition zones around the sutures. The inhibition-zone diameter was estimated from the original agar image using ImageJ software for the representative tested plate. Since independent replicate plates were not available, the antibacterial result was treated as a preliminary semi-quantitative observation rather than a statistically analyzed inhibition-zone study.

In vitro release behavior of the Co-Amoxiclav-loaded composite sutures was studied using PBS. A suture specimen weighing 0.1280 g was placed in 100 mL of PBS. The release medium was tested at pH 7.3 and pH 5.2 under identical conditions. At each selected time point of 1, 2, 3, 4, 5, 6, 7, and 8 h, 3 mL of the release medium was withdrawn and analyzed by ultraviolet-visible (UV-Vis) spectroscopy at 227 nm, and the withdrawn volume was replaced with an equal volume of fresh PBS. Quantification was performed using calibration curves prepared from serial dilutions of the same commercial Co-Amoxiclav formulation, and the concentrations were expressed as amoxicillin-equivalent values based on the labeled amoxicillin content of the formulation. The calibration range was 3-100 μg/mL, with correlation coefficients of R^2 = 0.9899 at pH 7.3 and R^2 = 0.9948 at pH 5.2. Since the drug loading capacity and loading efficiency were not directly measured, the release profile was interpreted as cumulative amoxicillin-equivalent release under the tested conditions.

6.5 Phosphate-buffered saline immersion mass-loss and photocatalytic evaluation

PBS immersion mass-loss behavior was evaluated by immersing the fabricated sutures in PBS. The percentage mass loss was calculated from the dry mass of the sample before immersion and the dry mass after immersion and drying at each selected time interval. The measured mass loss was interpreted as the combined effect of water penetration, leaching or dissolution of soluble components, PLA-associated hydrolytic changes, and possible loss of weakly

attached surface material, rather than as complete degradation of the PP/PLA matrix.

The photocatalytic activity was assessed by the degradation of MB solution under the UV light with the fabricated sutures. To determine the surface activity of the ZnO NPs associated with the UV degradation, the degradation efficiency was calculated. This test was deemed a secondary functional test and was not used directly to determine surgical eligibility.

6.6 Cell-based biological evaluation

The 3-(4,5-dimethylthiazol-2-yl)-2,5-diphenyltetrazolium bromide (MTT) assay was used to assess the cytotoxicity of the developed sutures with MCF-7 cells. Suture extracts were added to cells in 96 well plates at 1×10^4 cells/well, and cultured in RPMI-1640 medium containing 10% fetal bovine serum and antibiotics. MTT solution was added after 72 h of treatment and dimethyl sulfoxide (DMSO) was used to dissolve the formazan crystals that were formed. The absorbance was taken at 492 nm and the assay was repeated three times. The inhibition rate was determined from Eq. (1) [19]:

$$\textit{Inhibition rate (\%)} = [(A-B) / A] \times 100 \quad (1)$$

where, A = optical density of untreated control cells, and B = optical density of treated cells. Data were statistically analyzed using unpaired t-test analyzed by GraphPad Prism 6 and presented as mean ± standard deviation.

MCF-10A was used for preliminary biocompatibility response evaluation. The viability of the cells after exposure to the extracts from the sutures was determined. The biological tests were not considered to be a surgical-suture safety test but rather a preliminary cell-response screening test.

7. RESULTS AND DISCUSSION

7.1 Effect of poly (lactic acid) addition

Table 2 presents the mechanical properties and wettability of the surface of PP-based sutures with different PLA contents. Pure PP had high elongation (241 ± 2%) and also had high contact angle value of 125.066° which is indicative of its hydrophobic nature. The incorporation of PLA led to a decrease in the contact angle of the blends suggesting that the blends were more wettable, but with mechanical behavior changes.

Table 2. Effect of poly (lactic acid) (PLA) content on the mechanical properties and wettability of polymeric sutures

PP (wt.%)	PLA (wt.%)	CA (°)	TS (MPa)	TE (%)	E (GPa)
100	0	125.066	42 ± 1	241 ± 2	0.82 ± 0.05
75	25	62.769	45 ± 1	43 ± 2	0.93 ± 0.05
50	50	58.906	51 ± 1.5	53 ± 2	2.2 ± 0.1
25	75	41.644	30 ± 1	15 ± 1	0.65 ± 0.05

Note: Data are presented as mean ± standard deviation (n = 3). PP = Polypropylene, PLA = poly (lactic acid); CA = contact angle; TS = tensile strength, TE = total elongation, E = elastic modulus.

The contact angle of the PP/PLA 25/75 blend was the lowest (41.644°) while the tensile strength and elongation were significantly reduced to 30 ± 1 MPa and 15 ± 1%, respectively. However, the 50/50 blend gave the best overall balance, and it had the highest tensile strength of all the blends (PP/PLA) (51 ± 1.5 MPa), a high elastic modulus (2.2 ± 0.1 GPa), acceptable elongation (53 ± 2%) and significantly reduced contact angle compared to PP. The PP/PLA 50/50 blend was thus chosen as the base matrix for the next formulation steps, despite not having the lowest contact angle, due to the mechanical/wettability compromise.

7.2 Effect of polypropylene-grafted maleic anhydride addition

The effect of PP-g-MA content on the mechanical properties and surface wettability of the selected PP/PLA blend is shown in Table 3. The incorporation of PP-g-MA improved the compatibility of the PP/PLA blend, as reflected by the increase in tensile strength, elongation, and elastic modulus compared with the blend without compatibilizer.

Increasing the PP-g-MA content from 1 to 2 wt.% increased the tensile strength from 53 ± 1 to 58 ± 1.5 MPa and the elongation from 55 ± 2 to 76 ± 2%, while maintaining a high elastic modulus of 2.21 ± 0.10 GPa. This improvement can be attributed to enhanced interfacial adhesion between the PP and PLA phases. Although 4 wt.% PP-g-MA produced the lowest contact angle (58.801°) and a slightly higher modulus, the tensile strength and elongation decreased to 49 ± 1 MPa and 61 ± 2%, respectively. Therefore, 2 wt.% PP-g-MA was selected for the next formulation step because it provided the best mechanical balance, rather than the lowest contact-angle value.

Table 3. Effect of PP-g-MA content on the mechanical properties and wettability of polymeric sutures

PP-g-MA (wt.%)	CA (°)	TS (MPa)	TE (%)	E (GPa)
1	65.352	53 ± 1	55 ± 2	1.83 ± 0.05
2	62.525	58 ± 1.5	76 ± 2	2.21 ± 0.10
4	58.801	49 ± 1	61 ± 2	2.23 ± 0.10

Note: Data are presented as mean ± standard deviation (n = 3). PP-g-MA = Polypropylene-grafted maleic anhydride; CA = contact angle; TS = tensile strength, TE = total elongation, E = elastic modulus.

7.3 Effect of collagen addition

The effect of collagen content on the mechanical properties and surface wettability of the developed sutures is shown in Table 4. The incorporation of collagen improved the mechanical performance of the formulation up to 5 wt.%, while also reducing the contact angle compared with the previous formulation stage.

At 5 wt.% collagen, the suture showed the highest tensile strength (63 ± 1.5 MPa), total elongation of 62 ± 2%, and elastic modulus of 2.28 ± 0.10 GPa. This improvement may be attributed to the contribution of collagen functional groups to interfacial interaction within the polymer blend, which enhanced stress transfer through the composite structure. Increasing the collagen content to 7.5 wt.% further reduced the contact angle to 44°, indicating higher surface wettability; however, the tensile strength and elongation decreased to 56 ±

1 MPa and 54 ± 2%, respectively. This reduction may be related to excessive collagen loading, which can disturb matrix continuity or create less effective stress-transfer regions. Therefore, 5 wt.% collagen was selected for the next formulation step because it provided the best mechanical balance with improved wettability, rather than the lowest contact-angle value.

Table 4. Effect of collagen content on the mechanical properties and wettability of polymeric sutures

Collagen (wt.%)	CA (°)	TS (MPa)	TE (%)	E (GPa)
2.5	55	58 ± 1	60 ± 2	2.25 ± 0.10
5	49	63 ± 1.5	62 ± 2	2.28 ± 0.10
7.5	44	56 ± 1	54 ± 2	2.18 ± 0.10

Note: Mechanical data are presented as mean ± standard deviation (n = 3). CA = contact angle; TS = tensile strength, TE = total elongation, E = elastic modulus.

7.4 Effect of chitosan addition

The mechanical properties and surface wettability of the sutures developed are shown as a function of the chitosan content in Table 5. The contact angle decreased with the increase of chitosan content as this revealed better surface wettability, but the mechanical response was not found to increase with the increase of chitosan.

The suture with the highest tensile strength (66 ± 1.5 MPa) and elastic modulus (2.30 ± 0.10 GPa) was the one with the greatest chitosan concentration (2 wt.%). The elongation was acceptable (57 ± 2%) and the contact angle was reduced to 42° at this concentration. This improvement can be attributed to the improvement of the interaction between chitosan and polymer blend that led to the better transfer of stress in the composite structure. The contact angle was further decreased to 38° with 3 wt.% chitosan, but the tensile strength, elongation and elastic modulus decreased to 61 ± 1 MPa, 49 ± 2% and 2.15 ± 0.10 GPa, respectively. This decrease can be explained by the fact that the amount of chitosan loaded was too high, which can cause the continuity of the matrix to be disturbed, and the stress transfer area to be less effective. So, 2 wt.% chitosan was chosen for the next formulation step, as it offered the best mechanical balance with a good wettability, but not the lowest contact-angle.

Table 5. Effect of chitosan content on the mechanical properties and wettability of polymeric sutures

Chitosan (wt.%)	CA (°)	TS (MPa)	TE (%)	E (GPa)
1	46	64 ± 1	59 ± 2	2.24 ± 0.10
2	42	66 ± 1.5	57 ± 2	2.30 ± 0.10
3	38	61 ± 1	49 ± 2	2.15 ± 0.10

Note: Mechanical data are presented as mean ± standard deviation (n = 3). CA = contact angle; TS = tensile strength, TE = total elongation, E = elastic modulus.

7.5 Effect of polyethylene glycol addition

The effect of PEG content on the mechanical properties and surface wettability of the developed sutures is shown in Table 6. PEG addition slightly increased flexibility and wettability because of its plasticizing and hydrophilic nature.

The contact-angle values were very close for all PEG-containing formulations, decreasing slightly from 41.528° at 2.5 wt.% PEG to 41.176° at 7.5 wt.% PEG. However, higher PEG contents gradually reduced tensile strength and elastic modulus. At 2.5 wt.% PEG, the suture maintained the highest tensile strength (66 ± 1 MPa) and elastic modulus (2.12 ± 0.10 GPa), with acceptable elongation (62 ± 0.5%). Although 7.5 wt.% PEG produced slightly higher elongation and the lowest contact angle, it also showed lower strength and stiffness. Therefore, 2.5 wt.% PEG was selected for the next formulation step because it provided the best balance between mechanical stability and wettability.

Table 6. Effect of polyethylene glycol (PEG) content on the mechanical properties and wettability of polymeric sutures

PEG (wt.%)	CA (°)	TS (MPa)	TE (%)	E (GPa)
2.5	41.528	66 ± 1	62 ± 0.5	2.12 ± 0.10
5	41.275	64 ± 1.5	63.5 ± 0.5	2.05 ± 0.05
7.5	41.176	62 ± 1	65.5 ± 0.5	1.95 ± 0.05

Note: Mechanical data are presented as mean ± standard deviation (n = 3). PEG = polyethylene glycol; CA = contact angle; TS = tensile strength, TE = total elongation, E = elastic modulus.

7.6 Effect of zinc oxide addition

The effect of ZnO nanoparticle content on the mechanical properties and surface wettability of the developed sutures is shown in Table 7. The results show that increasing ZnO content improved surface wettability, as indicated by the decrease in contact angle from 56.818° at 1 wt.% ZnO to 50.285° at 1.5 wt.% ZnO and 45.225° at 2 wt.% ZnO. However, the mechanical performance did not follow the same monotonic trend, and the best reinforcement response was obtained at 1.5 wt.% ZnO.

At 1.5 wt.% ZnO, the suture showed the highest tensile strength (74.5 ± 0.5 MPa) and the highest elastic modulus (2.25 ± 0.05 GPa), while maintaining acceptable elongation (58.5 ± 0.5%) and improved wettability compared with the 1 wt.% ZnO formulation. This improvement may be attributed to the reinforcing effect of ZnO NPs at a suitable concentration, which can support stress transfer within the polymer-composite structure. Although 2 wt.% ZnO produced the lowest contact angle (45.225°), the tensile strength, elongation, and elastic modulus decreased compared with the 1.5 wt.% formulation. This reduction may be related to partial nanoparticle clustering or less effective stress transfer at higher ZnO loading. Therefore, 1.5 wt.% ZnO was selected as the reinforced formulation for subsequent evaluation because it provided the best mechanical performance with improved surface wettability.

Table 7. Effect of ZnO nanoparticle content on the mechanical properties and wettability of polymeric sutures

ZnO (wt.%)	CA (°)	TS (MPa)	TE (%)	E (GPa)
1	56.818	68.5 ± 1	60 ± 1	2.05 ± 0.05
1.5	50.285	74.5 ± 0.5	58.5 ± 0.5	2.25 ± 0.05
2	45.225	70 ± 1	56 ± 1	2.00 ± 0.10

Note: Mechanical data are presented as mean ± standard deviation (n = 3). Contact-angle values are reported as average values from surface-position measurements. CA = contact angle; TS = tensile strength, TE = total elongation, E = elastic modulus.

7.7 Physicochemical and functional characterization of the selected zinc oxide-reinforced suture

7.7.1 Field-emission scanning electron microscopy and Energy-dispersive X-ray spectroscopy analysis

The FESEM image and EDX spectrum of the selected unloaded ZnO-reinforced composite suture are shown in Figure 2. The unloaded suture exhibited a continuous fibrous morphology with a relatively rough surface, which may be associated with ZnO nanoparticle incorporation into the polymer-composite matrix. The observed ZnO-containing surface features were within the nanoscale range of approximately 29-50 nm.

The EDX spectrum in Figure 2 showed carbon, oxygen, and zinc signals. Carbon and oxygen are mainly related to the polymeric matrix and oxygen-containing components, while zinc indicates the presence of ZnO in the analyzed surface region. Minor Au peaks were attributed to the sputter-coating process [13].

The FESEM image and EDX spectrum of the Co-Amoxiclav-loaded ZnO-reinforced composite suture are shown in Figure 3. After drug loading, the suture maintained its continuous fibrous structure, indicating that the soaking-based loading process did not visibly damage the filament surface. The loaded sample appeared smoother than the unloaded one, probably because of partial coverage by the deposited Co-Amoxiclav/PVP layer. The observed surface features increased slightly to approximately 35-65 nm, which may be related to surface deposition and limited local aggregation.

The EDX spectrum in Figure 3 showed dominant carbon and oxygen signals, while the Zn signal was reduced or not clearly detected in the analyzed area. This behavior may indicate partial coverage of ZnO-containing regions by the deposited drug/PVP layer. Thus, FESEM/EDX provided qualitative evidence of surface morphology and elemental changes after loading; however, quantitative drug loading was not determined by EDX analysis [13].

7.7.2 Fourier transform infrared spectroscopy analysis

The FTIR spectra of the unloaded and Co-Amoxiclav-loaded ZnO-reinforced sutures are shown in Figure 4. The unloaded suture showed characteristic absorption bands at 2949, 2917, and 2836 cm^{-1}, corresponding to C-H stretching vibrations of the polymeric matrix. Additional bands at 1457 and 1375 cm^{-1} are related to C-H bending vibrations, while the bands in the range of 1169-841 cm^{-1} are associated with C-O/C-O-C and fingerprint-region vibrations of the polymer blend and incorporated additives. The band near 419 cm^{-1} supports the presence of Zn-O vibration.

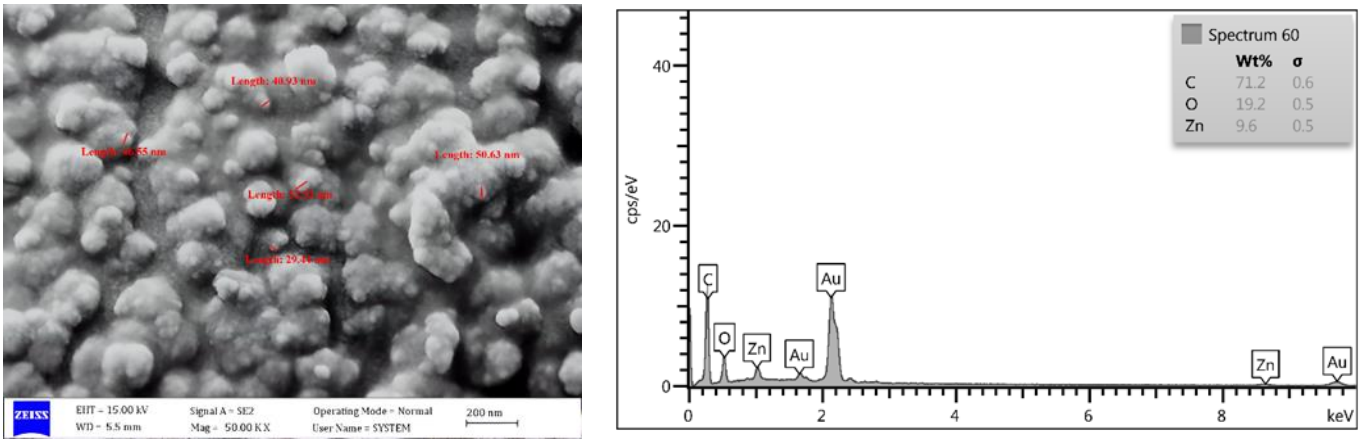

(a) (b)

Figure 2. Morphological and elemental analysis of the unloaded ZnO-reinforced composite suture: (a) field-emission scanning electron microscopy (FESEM) image, (b) energy-dispersive X-ray spectroscopy (EDX) spectrum

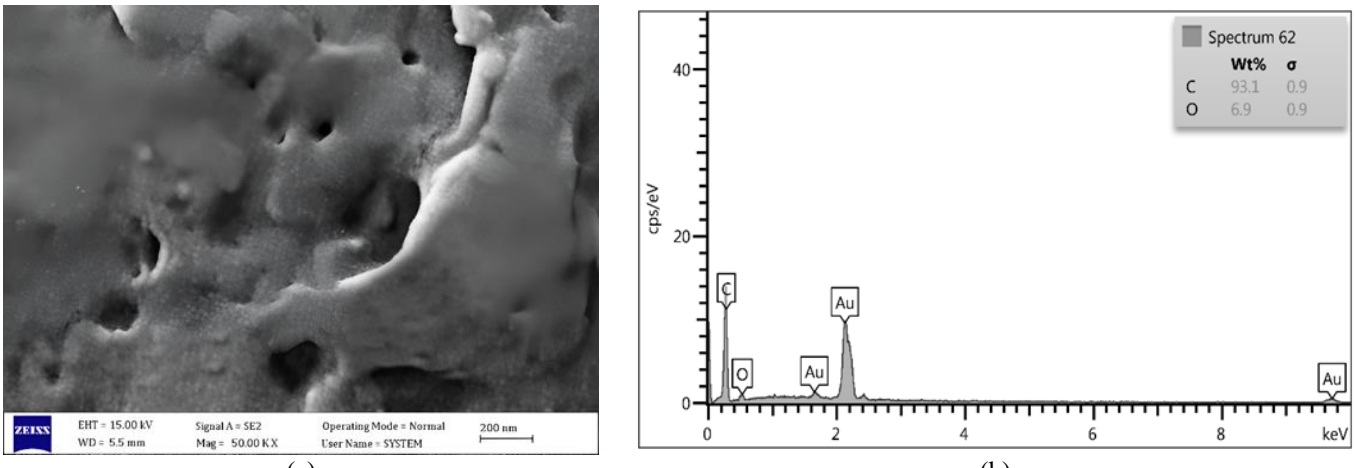

(a) (b)

Figure 3. Morphological and elemental analysis of the Co-Amoxiclav-loaded ZnO-reinforced composite suture: (a) field-emission scanning electron microscopy (FESEM) image, (b) energy-dispersive X-ray spectroscopy (EDX) spectrum

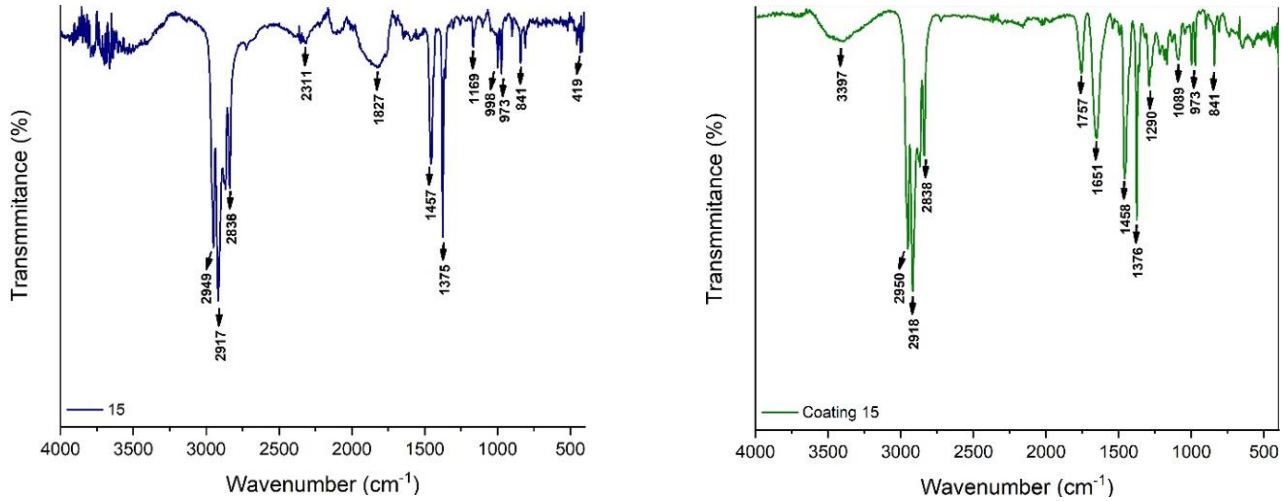

Figure 4. Fourier transform infrared spectroscopy (FTIR) spectra of the selected ZnO-reinforced composite suture: (a) unloaded suture, (b) Co-Amoxiclav-loaded suture

After Co-Amoxiclav loading, a broad band appeared around 3397 cm^{-1}, which can be assigned to O-H/N-H stretching. Additional bands at 1757, 1651, 1290, and 1099 cm^{-1} may be associated with carbonyl, amide-related, and C-O vibrations from the deposited Co-Amoxiclav/PVP layer. The main polymer-related bands remained visible after loading, with no major peak disappearance or strong shift, indicating that loading occurred mainly through physical deposition or weak interfacial interaction rather than formation of new strong chemical bonds [14].

7.7.3 Contact angle measurement

The contact-angle results of the selected unloaded and Co-Amoxiclav/PVP-loaded ZnO-reinforced sutures are shown in Figure 5. The selected unloaded ZnO-reinforced suture showed a contact angle of 50.285°, whereas the Co-Amoxiclav/PVP-loaded suture showed a slightly lower value of 48.8°, indicating a small improvement in surface wettability after loading.

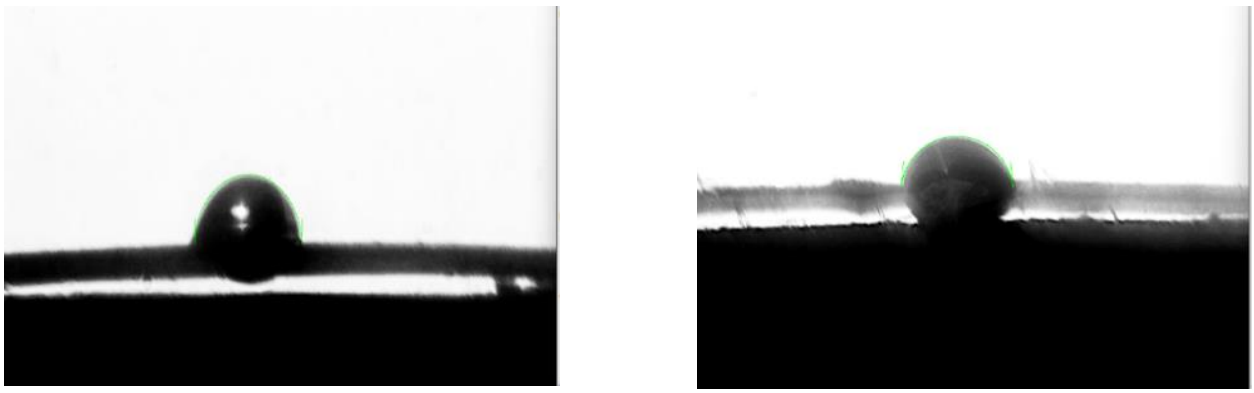

(a) (b)

Figure 5. Contact angle images of (a) unloaded, (b) Co-Amoxiclav/PVP-loaded ZnO-reinforced composite sutures

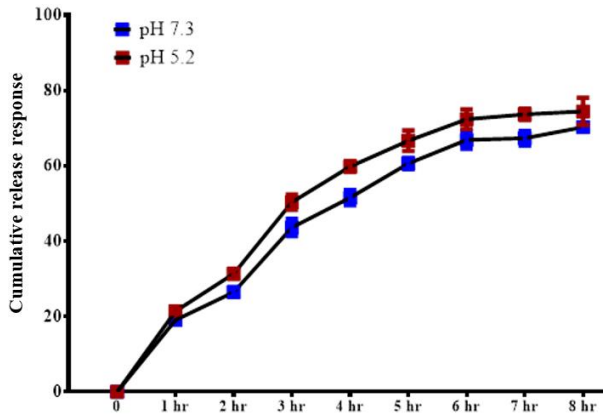

Figure 6. Cumulative amoxicillin-equivalent release profile of the Co-Amoxiclav-loaded ZnO-reinforced composite suture at pH 7.3 and pH 5.2

The slight decrease in contact angle after loading may be attributed to the deposited Co-Amoxiclav/PVP layer, which can increase the polar contribution at the suture surface and improve water affinity. Because the specimens had a cylindrical filament geometry, the values were interpreted as apparent water contact angles measured under the applied LBADSA setup using a distilled-water droplet of approximately 2.75 µL, rather than as absolute flat-surface wettability values. Therefore, the contact-angle result supports surface modification after loading, but it should not be considered direct evidence of improved in vivo biological performance [14].

7.7.4 Drug release study

The cumulative amoxicillin-equivalent release profiles of the Co-Amoxiclav-loaded ZnO-reinforced sutures at pH 7.3 and pH 5.2 are shown in Figure 6. The release increased

gradually with time, showing an initial faster release stage during the first hours followed by a slower release stage up to 8 h. This behavior is consistent with the general release pattern reported for coated or nanoparticle-assisted suture delivery systems [6, 20].

The initial release can be attributed to the diffusion of drug molecules located near or on the suture surface, while the slower stage may be related to diffusion from the deposited Co-Amoxiclav/PVP layer and the polymer-composite structure. The release at pH 5.2 was slightly higher than that at pH 7.3 throughout the test, which may be associated with the solubility behavior of amoxicillin and the swelling/leaching of the PVP-containing surface layer under acidic conditions [17].

By 8 h, the plotted cumulative amoxicillin-equivalent release response reached higher final values at pH 5.2 than at pH 7.3 under the same testing conditions. This pH-dependent difference indicates that the acidic medium promoted a slightly higher release response from the Co-Amoxiclav/PVP-loaded surface layer. Since the exact drug loading capacity and loading efficiency were not directly quantified, the release data should be used to compare the release behavior of the tested formulations under identical loading and testing conditions, rather than to represent the percentage of the total drug initially loaded into the suture.

7.7.5 Phosphate-buffered saline immersion mass-loss behavior

The PBS immersion mass-loss behavior of the Co-Amoxiclav-loaded ZnO-reinforced suture in PBS (pH 7.4) at 37 °C is shown in Table 8.

Table 8. Phosphate-buffered saline (PBS) immersion mass-loss behavior of Co-Amoxiclav-loaded ZnO-reinforced sutures in PBS (pH 7.4) at 37 °C

Time (Days)	Weight Loss (%)
7	21.8
14	43.7
21	60.8

Weight loss was calculated gravimetrically according to Eq. (2) [21]:

$$Weight\ loss\ (\%) = [(W_0 - W_t)/W_0] \times 100 \quad (2)$$

where, W_0 is the initial dry mass before immersion and W_t is the dry mass after immersion at each selected time interval.

After 7, 14, and 21 days of PBS immersion, the measured dry-mass loss reached 21.8%, 43.7%, and 60.8%, respectively. This progressive decrease in mass should be interpreted as PBS immersion mass-loss behavior rather than complete degradation of the PP/PLA matrix. The observed mass loss may result from combined contributions of water penetration, leaching or dissolution of soluble components such as PVP and the loaded drug, hydrolytic changes associated mainly with the PLA-containing phase, and possible loss of weakly attached surface components. Therefore, the mass-loss data indicate material changes during immersion, but they do not directly demonstrate retention or loss of mechanical support because tensile retention after immersion was not measured.

7.7.6 Photocatalytic activity

The photocatalytic activity of the Co-Amoxiclav loaded ZnO-reinforced suture was carried out by observing the degradation of MB as depicted in Figure 7. It can be seen that the absorption peak of MB dye is decreasing gradually with the time of irradiation which shows the degradation of the dye in the presence of the ZnO containing suture.

The degradation efficiency reached approximately 77% after 180 min. This behavior can be attributed to ZnO NPs, which can generate reactive oxygen species under UV exposure and contribute to oxidative dye degradation [22]. However, this test was considered an auxiliary indication of ZnO activity and should not be interpreted as direct evidence of surgical suitability, because wound-closure sutures are not normally exposed to UV irradiation during use.

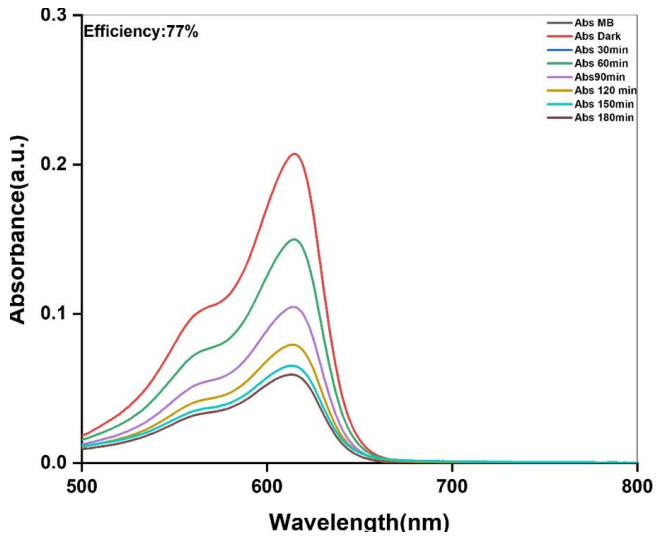

Figure 7. Ultraviolet-visible (UV-Vis) spectra of methylene blue degradation in the presence of the Co-Amoxiclav-loaded ZnO-reinforced composite suture under UV irradiation

7.8 Biological evaluation

7.8.1 Antibacterial activity

The antibacterial activity of the unloaded and Co-Amoxiclav-loaded ZnO-reinforced sutures against Staphylococcus aureus and Escherichia coli is shown in Figure 8. The agar diffusion results showed visible inhibition zones around the tested sutures, indicating antibacterial activity under the tested in vitro conditions.

The Co-Amoxiclav-loaded suture showed larger visible inhibition zones than the unloaded ZnO-reinforced suture under the tested agar diffusion conditions, which is consistent with the expected antibacterial contribution of the loaded Co-Amoxiclav formulation together with ZnO NPs and chitosan within the composite structure [6, 10, 15, 16]. Based on the representative original agar image, the inhibition-zone diameter around the loaded suture was estimated to be about 36 mm using ImageJ software. However, because independent replicate plates were not available, the antibacterial result was interpreted as a preliminary semi-quantitative observation and was not presented as mean ± standard deviation. Therefore, the antibacterial findings support the presence of in vitro antibacterial activity under the tested conditions, but further replicated tests with standardized controls are required for full quantitative confirmation.

7.8.2 3-(4,5-dimethylthiazol-2-yl)-2,5-diphenyltetrazolium bromide assay

The MTT response of MCF-7 cells after exposure to the ZnO-reinforced suture extract is shown in Figure 9. The

treated cells showed a reduced viability of 25.7 ± 1.5% compared with the untreated control, indicating that the suture extract affected MCF-7 cell metabolic activity under the tested in vitro conditions.

Microscopic observation showed changes in cell morphology, including reduced cell density, cell shrinkage, and partial detachment from the culture surface. This response may be associated with ZnO-related oxidative stress, which can reduce cell viability [11]. However, since MCF-7 is a cancer cell line and not a normal, wound-relevant cell type, this assay was considered an auxiliary assessment of cell-response and not as a sole test to determine surgical-suture biocompatibility or clinical suitability.

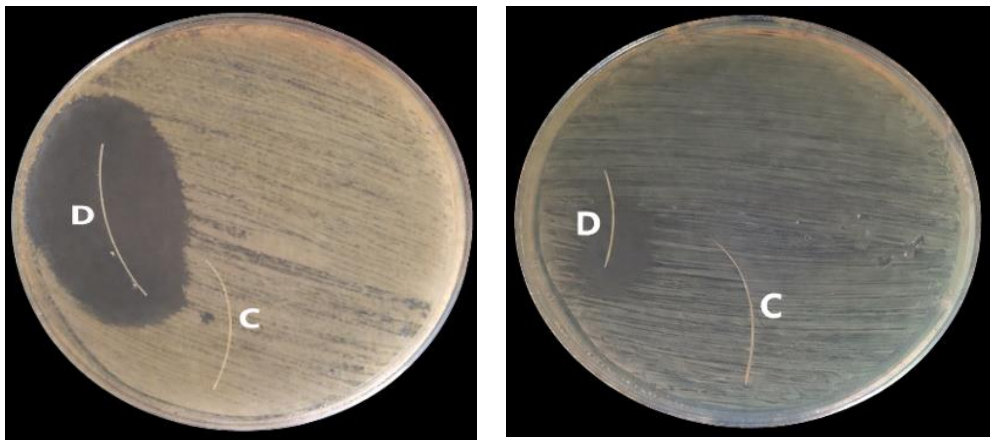

(a) (b)

Figure 8. Antibacterial activity of unloaded and Co-Amoxiclav-loaded ZnO-reinforced composite sutures against Staphylococcus aureus and Escherichia coli

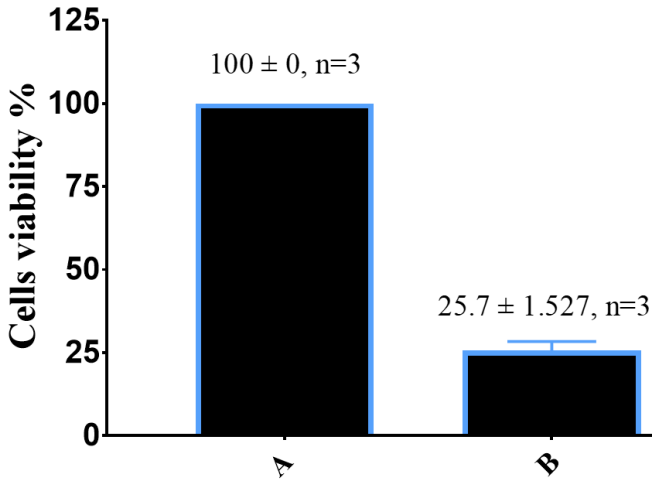

Figure 9. 3-(4,5-dimethylthiazol-2-yl)-2,5-diphenyltetrazolium bromide (MTT) response and morphological observation of MCF-7 cells after exposure to the ZnO-reinforced suture extract: (a) untreated control cells, (b) treated cells

7.8.3 Biocompatibility evaluation

The response of MCF-10A cell is given in Figure 10 following exposure to the ZnO-reinforced suture extract. The viability of the treated cells was 90.85 ± 0.83% suggesting that the extract was not very toxic to MCF-10A cells when tested under the in vitro conditions.

The cells cultured in the treated samples were observed under the microscope and were found to have a morphology similar to the untreated control with no apparent shrinkage, damage to the cell surface and no significant decrease in cell density. This response might be due to the stable incorporation of the ZnO NPs inside the polymer-composite matrix which can decrease the effects of oxidative stress due to the reduction of excessive release of NPs [11]. These results, however, are preliminary cytocompatibility results and should not be considered as proof of surgical-suture biocompatibility since MCF-10A is a single normal epithelial cell line. Further evaluation using wound-relevant cells, hemocompatibility and inflammatory-response assays, and standardized ISO 10993 testing is required before surgical applicability can be claimed [23].

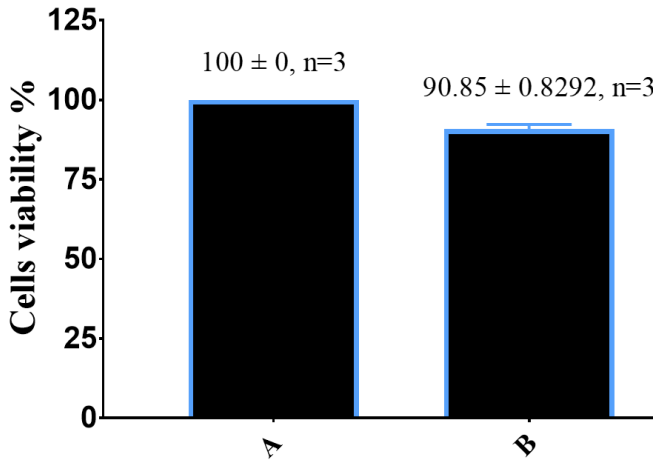

Figure 10. MCF-10A cell response after exposure to the ZnO-reinforced suture extract: (a) untreated control cells, (b) treated cells

8. CONCLUSIONS

This study developed ZnO-reinforced Co-Amoxiclav-loaded PP/PLA composite sutures using a stepwise formulation screening approach. The selected composition, consisting of a 50/50 PP/PLA matrix with 2 wt.% PP-g-MA, 5 wt.% collagen, 2 wt.% chitosan, 2.5 wt.% PEG, and 1.5 wt.% ZnO NPs, provided the most suitable balance among the tested formulations. The selected suture showed a tensile strength of 74.5 ± 0.5 MPa, elastic modulus of 2.25 ± 0.05 GPa, and elongation of 58.5 ± 0.5%. FESEM/EDX, FTIR, and contact-

angle analyses supported ZnO incorporation, surface modification after Co-Amoxiclav/PVP loading, and improved apparent wettability. The loaded sutures showed progressive amoxicillin-equivalent release over 8 h, PBS immersion mass loss reaching 60.8% after 21 days, and 77% methylene blue degradation under UV irradiation. Antibacterial testing showed visible inhibition zones, with the loaded suture showing larger visible zones than the unloaded suture, while cell-based assays showed reduced MCF-7 viability and high MCF-10A viability under the tested in vitro conditions. Overall, the developed composite suture demonstrated promising material-level performance; however, further studies on quantitative drug loading, tensile retention after PBS immersion, standardized antibacterial controls, wound-relevant cells, hemocompatibility, inflammatory response, sterilization validation, and ISO 10993-based testing are required before surgical applicability can be claimed.

ACKNOWLEDGMENT

The authors would like to express their sincere appreciation to the Department of Polymer Engineering and Petrochemical Industries, College of Materials Engineering, University of Babylon, Iraq, for providing laboratory facilities and technical support that contributed to the completion of this work.

REFERENCES

[1] Duarte-Peña, L., Fragoso-Medina, A.J., Bucio, E., López-Saucedo, F. (2023). Improving the therapeutic value of sutures. Advanced Technologies and Polymer Materials for Surgical Sutures, pp. 45-76. https://doi.org/10.1016/B978-0-12-819750-9.00003-6

[2] Xu, L., Liu, Y.N., Zhou, W.H., Yu, D.G. (2022). Electrospun medical sutures for wound healing: A review. Polymers, 14(9): 1637. https://doi.org/10.3390/polym14091637

[3] Afewerki, S., Bassous, N., Harb, S., Palo-Nieto, C., Ruiz-Esparza, G.U., Marciano, F.R., Webster, T.J., Furtado, A.S.A., Lobo, A.O. (2020). Advances in dual functional antimicrobial and osteoinductive biomaterials for orthopaedic applications. Nanomedicine: Nanotechnology, Biology and Medicine, 24: 102143. https://doi.org/10.1016/j.nano.2019.102143

[4] Han, G.Y., Hwang, S.K., Cho, K.H., Kim, H.J., Cho, C.S. (2023). Progress of tissue adhesives based on proteins and synthetic polymers. Biomaterials Research, 27(1): 57. https://doi.org/10.1186/s40824-023-00397-4

[5] Makrygiannis, I.H., Nikolaidis, A.K., Tilaveridis, I., Kouvelas, A.D., Lykakis, I.N., Venetis, G. (2025). Coated sutures for use in oral surgery: A comprehensive review. In Clinical Oral Investigations, 29(2): 109. https://doi.org/10.1007/s00784-025-06176-w

[6] Sampathi, S., Tiriya, P.K., Dodoala, S., Junnuthula, V., Dyawanapelly, S. (2022). Development of biocompatible ciprofloxacin-gold nanoparticle coated sutures for surgical site infections. Pharmaceutics, 14(10): 2130. https://doi.org/10.3390/pharmaceutics14102130

[7] Li, X.G., Yang, Q., Zhang, K., Pan, L.S., Feng, Y.H., Jia, Y.F., Xu, N. (2022). Property improvement and compatibilization mechanism of biodegradable polylactic acid/maleic anhydride-based/polypropylene spunbonded nonwoven slices. Journal of Cleaner Production, 375: 134097. https://doi.org/10.1016/j.jclepro.2022.134097

[8] Huang, H.M. (2020). Medical application of polymer-based composites. Polymers, 12(11): 2560. https://doi.org/10.3390/polym12112560

[9] Tang, W.D., He, G.J., Huang, W.T., Zou, X.L., Cao, X.W., Yin, X.C. (2021). The reactive compatibilization of PLA/PP blends and improvement of PLA crystallization properties induced by in situ UV irradiation. CrystEngComm, 23(4): 864-875. https://doi.org/10.1039/D0CE01445A

[10] Khashan, K.S., Badr, B.A., Sulaiman, G.M., Jabir, M.S., Hussain, S.A. (2021). Antibacterial activity of Zinc Oxide nanostructured materials synthesis by laser ablation method. Journal of Physics: Conference Series, 1795(1): 012040. https://doi.org/10.1088/1742-6596/1795/1/012040

[11] Alyamani, A.A., Al-Musawi, M.H., Albukhaty, S., Sulaiman, G.M., et al. (2023). Electrospun polycaprolactone/chitosan nanofibers containing Cordia myxa fruit extract as potential biocompatible antibacterial wound dressings. Molecules, 28(6): 2501. https://doi.org/10.3390/molecules28062501

[12] Shah, J., Patel, D., Rananavare, D., Hudson, D., Tran, M., Schloss, R., Langrana, N., Berthiaume, F., Kumar, S. (2025). Recent advancements in chitosan-based biomaterials for wound healing. Journal of Functional Biomaterials, 16(2): 45. https://doi.org/10.3390/jfb16020045

[13] Shebl, H.R., Soliman, R.A., Abdallah, O.M. (2025). An in vitro study on the efficacy of nanoparticles and nanocomposites as coating materials on surgical sutures. Scientific Reports, 15(1): 20368. https://doi.org/10.1038/s41598-025-07558-6

[14] Safari, P., Rahimabadi, E.Z., Vaezi, M.R., Behnamghader, A., Tahergorabi, R. (2025). Development of ZnO-NPs reinforced chitosan nanofiber mats with improved antibacterial and biocompatibility properties. Scientific Reports, 15(1): 16567. https://doi.org/10.1038/s41598-025-01669-w

[15] Monroy Caltzonci, D.A., Rasu Chettiar, A.D., Ibarra, V.C., Marasamy, L., Loredo-Tovías, M., Acosta-Torres, L.S., Manisekaran, R. (2024). Antimicrobial and cytotoxic effect of positively charged nanosilver-coated silk sutures. ACS Omega, 9(15): 17636-17645. https://doi.org/10.1021/acsomega.4c01257

[16] Blinov, A.V., Nagdalian, A.A., Povetkin, S.N., Gvozdenko, A.A., et al. (2022). Surface-oxidized polymer-stabilized silver nanoparticles as a covering component of suture materials. Micromachines, 13(7): 1105. https://doi.org/10.3390/mi13071105

[17] Ibne Shoukani, H., Nisa, S., Bibi, Y., Zia, M., Sajjad, A., Ishfaq, A., Ali, H. (2024). Ciprofloxacin loaded PEG coated ZnO nanoparticles with enhanced antibacterial and wound healing effects. Scientific Reports, 14(1): 4689. https://doi.org/10.1038/s41598-024-55306-z

[18] Pagnanelli, M., De Gaetano, F., Nappo, G., Capretti, G., Costantino, M.L., Zerbi, A. (2023). The choice of the most appropriate suture threads for pancreatic anastomoses on the basis of their mechanical characteristics. Biomedicines, 11(4): 1055. https://doi.org/10.3390/biomedicines11041055

[19] Abduladheem, J.R., Neima, H.N. (2021). Investigation of antioxidant and cytotoxicity effects of silver nanoparticles produced by biosynthesis using lactobacillus gasseri. Archives of Razi Institute, 76(5): 81-793. https://doi.org/10.22092/ari.2021.355949.1747
[20] Zhou, Y.L., Yang, Q.Q., Zhang, L.Z., Tang, J.B. (2021). Nanoparticle-coated sutures providing sustained growth factor delivery to improve the healing strength of injured tendons. Acta Biomaterialia, 124: 301-314. https://doi.org/10.1016/j.actbio.2021.01.008
[21] Puglisi, R., Scamporrino, A.A., Dintcheva, N.T., Filippone, G., Bruno, E., Scarfato, P., Cerruti, P., Carroccio, S.C. (2023). Photo- and water-degradation phenomena of ZnO bio-blend based on poly(lactic acid) and polyamide 11. Polymers, 15(6): 1434. https://doi.org/10.3390/polym15061434
[22] Abu-Dalo, M.A., Al-Rosan, S.A., Albiss, B.A. (2021). Photocatalytic degradation of methylene blue using polymeric membranes based on cellulose acetate impregnated with ZnO nanostructures. Polymers, 13(19): 3451. https://doi.org/10.3390/polym13193451
[23] Barbosa, M.C.D.S., Silva, H.N.D., Lopes, D.D.S., Wanderley, W.F., Rosendo, R.A., Penha, E.S.D., Barbosa, R.C., Soares, M.F.D.L.R., Sobrinho, J.L.S., Fook, M.V.L. (2024). Biodegradable chitosan sutures enhanced with N-acetyl-D-glucosamine: Comparative Study with catgut sutures. Materials Research, 27: e20240278. https://doi.org/10.1590/1980-5373-MR-2024-0278

NOMENCLATURE

A	optical density of untreated control cells in the MTT assay, dimensionless
ASTM	ASTM International
B	optical density of treated cells in the MTT assay, dimensionless
CA	apparent water contact angle, degree
CCD	charge-coupled device
Co-Amoxiclav	commercial amoxicillin/clavulanic-acid formulation
DMSO	dimethyl sulfoxide
E	elastic modulus, GPa
EDX	energy-dispersive X-ray spectroscopy
FESEM	field-emission scanning electron microscopy
FTIR	Fourier transform infrared spectroscopy
ISO	International Organization for Standardization
LBADSA	low-bond axisymmetric drop shape analysis
MB	methylene blue
MCF-10A	Michigan Cancer Foundation-10A
MCF-7	Michigan Cancer Foundation-7
MTT	3-(4,5-dimethylthiazol-2-yl)-2,5-diphenyltetrazolium bromide
n	number of replicate measurements
NPs	nanoparticles
PBS	phosphate-buffered saline
PEG	polyethylene glycol
pH	negative logarithm of hydrogen ion activity
PLA	poly(lactic acid)
PP	polypropylene
PP-g-MA	polypropylene-grafted maleic anhydride
PVP	polyvinylpyrrolidone
RPMI-1640	Roswell Park Memorial Institute 1640 medium
t	time, min/h/days
TE	total elongation, %
TS	tensile strength, MPa
UV	ultraviolet
UV-Vis	ultraviolet-visible
W_0	initial dry mass before immersion, g
W_t	dry mass after immersion, g
wt.%	mass fraction, dimensionless
ZnO	zinc oxide

Subscripts

0	initial value before immersion
t	the selected time interval